

HHV-7 U21 exploits Golgi quality control carriers to reroute class I MHC molecules to lysosomes

Aaron T. Dirck, Melissa L. Whyte, and Amy W. Hudson*

Department of Microbiology and Immunology, Medical College of Wisconsin, Milwaukee, WI 53226

ABSTRACT The human herpesvirus-7 (HHV-7) U21 glycoprotein binds to class I major histocompatibility complex (MHC) molecules in the endoplasmic reticulum (ER) and reroutes them to lysosomes. How this single viral glycoprotein efficiently redirects the U21/class I MHC complex to the lysosomal compartment is poorly understood. To investigate the trafficking of HHV-7 U21, we followed synchronous release of U21 from the ER as it traffics through the secretory system. Sorting of integral membrane proteins from the *trans*-Golgi network (TGN) has been shown to occur through tubular carriers that emanate from the TGN or through vesicular carriers that recruit GGA (Golgi-localized, γ -ear-containing, ARF-binding protein), clathrin adaptors, and clathrin. Here, we present evidence for the existence of a third type of Golgi-derived carrier that is vesicular, yet clathrin independent. This U21-containing carrier also carries a Golgi membrane protein engineered to form inducible oligomers. We propose that U21 employs the novel mechanism of forming oligomeric complexes with class I MHC molecules that result in sorting of the oligomeric U21/class I MHC complexes to Golgi-derived quality control carriers destined for lysosomes.

Monitoring Editor

Benjamin Glick
University of Chicago

Received: Jul 8, 2019

Revised: Nov 22, 2019

Accepted: Dec 6, 2019

INTRODUCTION

Viruses can provide excellent tools for the study of cell biological processes involved in membrane trafficking, as many viruses have evolved means to alter trafficking of integral membrane proteins in an effort to avoid detection by the host (for review, see Alcami and Koszinowski, 2000; Tortorella *et al.*, 2000). Several herpesviral gene products strategically impair the intracellular trafficking of host immune recognition or signaling molecules to reduce the presence of these molecules on the plasma membrane (Douglas *et al.*, 2010).

This article was published online ahead of print in MBoC in Press (<http://www.molbiolcell.org/cgi/doi/10.1091/mbc.E19-07-0363>) on December 18, 2019.

The authors declare no competing financial interests.

*Address correspondence to: Amy W. Hudson (ahudson@mcw.edu).

Abbreviations used: BSA, bovine serum albumin; CARTS, carriers of the TGN to the cell surface; CDMPR, cation-dependent mannose 6-phosphate receptor; eGFP, enhanced green fluorescent protein; ER, endoplasmic reticulum; FBS, fetal bovine serum; GalT, galactosyl transferase; GGA, Golgi-localized, γ -ear-containing, ARF-binding protein; HHV-7, human herpesvirus-7; lamp1, lysosome-associated membrane protein-1; ManI, mannosidase I; MHC, major histocompatibility complex; PBS, phosphate-buffered saline; QC carriers, quality control carriers; RUSH, retention using selective hooks; SBP, streptavidin-binding peptide; SIM, structured illumination microscopy; TfR, transferrin receptor; TGN, *trans*-Golgi network; TNF α , tumor necrosis factor- α ; VSV-G, vesicular stomatitis virus envelope glycoprotein.

© 2020 Dirck *et al.* This article is distributed by The American Society for Cell Biology under license from the author(s). Two months after publication it is available to the public under an Attribution–Noncommercial–Share Alike 3.0 Unported Creative Commons License (<http://creativecommons.org/licenses/by-nc-sa/3.0>).

“ASCB®,” “The American Society for Cell Biology®,” and “Molecular Biology of the Cell®” are registered trademarks of The American Society for Cell Biology.

We have previously shown that the U21 gene product from human herpesvirus-7 (HHV-7) binds to newly synthesized class I major histocompatibility complex (MHC) molecules in the endoplasmic reticulum (ER) and reroutes them to lysosomes, where both proteins are degraded (Hudson *et al.*, 2001; May *et al.*, 2014). Although U21 lacks sequence similarity to any other protein, multiple structural threading algorithms predict that U21 itself possesses a class I MHC-like protein fold (May *et al.*, 2014). While progress has been made in determining how this class I MHC-like viral protein can so effectively reroute class I molecules to lysosomes, its lysosomal sorting mechanism remains a mystery.

Trafficking of integral membrane proteins to the lysosome/late endosomal compartment is generally mediated by proteins that recognize cytoplasmic tyrosine- or dileucine-based sorting signals (for review, see Braulke and Bonifacio, 2009). In the simplest model for U21-mediated trafficking of class I MHC molecules to lysosomes, U21 would contain a sorting signal in its cytoplasmic tail. Surprisingly, we found that the cytoplasmic tail of U21 was entirely dispensable and that the soluble luminal domain of U21 was sufficient to reroute class I molecules to the lysosomal compartment (Glosson *et al.*, 2010). Sorting information contained within U21 must therefore be located within the luminal portion of U21. Our working model for U21's ability to reroute class I MHC molecules invokes the association of U21 with some as yet unknown cellular sorting protein that contains a conventional lysosomal sorting motif in its

cytoplasmic tail. This sorting motif, in turn, would recruit adaptor molecules that mediate the trafficking of the U21-class I complex to late endosomes and, eventually, lysosomes (Glosson *et al.*, 2010).

Lysosomal membrane proteins traffic to lysosomes either via a direct route, from the *trans*-Golgi network (TGN) to endosomes and lysosomes without reaching the plasma membrane, or an indirect route to the plasma membrane first, and then trafficking to lysosomes via the endosomal system (for review, see Kornfeld and Mellman, 1989; Hunziker and Geuze, 1996; Bralke and Bonifacino, 2009). In most cases, the fraction of a particular lysosomal membrane protein that traffics via the direct or the indirect route has not been definitively determined. For the lysosome-associated membrane protein-1 (lamp1), depletion of the clathrin adaptor protein complex AP-2, which is associated with internalized plasma membrane-derived vesicles, results in accumulation of lamp1 on the plasma membrane, suggesting that a significant fraction of lamp1 traffics via the plasma membrane en route to lysosomes (Janvier and Bonifacino, 2005). Like lamp1, U21 is localized in lysosomes at steady state. Unlike lamp1, U21 has the ability to reroute class I MHC molecules to lysosomes, and this is unaffected by depletion of AP-2, while depletion of AP-1 and AP-3 has a dramatic effect, suggesting that U21 traffics to lysosomes predominantly via the direct route (Kimpler *et al.*, 2014).

In this study, to directly monitor progression of U21 through the secretory pathway, we employed the method of retention using selective hooks (RUSH), which allows synchronous release and visualization of cargo through the secretory pathway. In this system, Boncompain *et al.* (2012) fused several “reporter” molecules—lamp1, tumor necrosis factor- α (TNF α), e-cadherin, and vesicular stomatitis virus envelope glycoprotein (VSV-G)—to streptavidin-binding peptide (SBP) and a fluorescent protein tag (enhanced green fluorescent protein [eGFP] or mCherry). These reporter molecules are retained in the ER when coexpressed with ER-retained “hook” proteins—either streptavidin fused to the luminal ER retention signal KDEL or streptavidin fused to the cytoplasmic tail of an invariant chain mutant that is retained in the ER. Addition of biotin to the cells releases the hooked proteins from the streptavidin in synchrony, and the fluorescent proteins can be imaged using live microscopy (Boncompain *et al.*, 2012) (Figure 1a). Using RUSH, Chen *et al.* (2017) examined the trafficking of three integral membrane proteins with different steady-state distributions in the endolysosomal system, monitoring the synchronous release of the lysosomal integral membrane protein lamp1, the TGN-localized cation-dependent mannose 6-phosphate receptor (CDMPR), and the plasma membrane–recycling transferrin receptor (TfR) from the ER. Exit of CDMPR in these vesicular transport carriers is dependent upon a cytosolic dileucine-based signal that interacts with GGA adaptors (Puertollano *et al.*, 2001; Zhu *et al.*, 2001; Chen *et al.*, 2017), and these CDMPR-containing vesicular carriers transit directly to the endolysosomal pathway (for review, see Kornfeld and Mellman, 1989; Hunziker and Geuze, 1996; Bralke and Bonifacino, 2009). TfR, VSV-G, and lamp1, on the other hand, segregate from CDMPR-containing vesicles in the Golgi and exit the Golgi in tubules, without dependence upon cytoplasmic sorting signals (Chen *et al.*, 2017). Each of these proteins is destined for the plasma membrane (Hirschberg *et al.*, 1998; Polishchuk *et al.*, 2000; Chen *et al.*, 2017; for review, see Bard and Malhotra, 2006). Clathrin adaptor AP-2 molecules are then recruited to the cytoplasmic tails of TfR and lamp1 at the plasma membrane, where endocytosis and subsequent sorting to lysosomes or recycling endosomes ensues (Chen *et al.*, 2017). Chen *et al.* (2017) found that the CDMPR, which is notable for taking the direct route to lysosomes, is sequestered from

TfR and lamp1 in the Golgi complex before export of the molecules to the plasma membrane; interestingly, TfR and lamp molecules exit from the Golgi in tubules, while CDMPR leaves the Golgi in vesicles (Polishchuk *et al.*, 2003; Chen *et al.*, 2017).

In an effort to uncover clues as to the mode of lysosomal trafficking employed by U21 as it reroutes class I MHC molecules to lysosomes, we employed RUSH to compare the trafficking of U21 to that of lamp1, CDMPR, and other plasma membrane–localized integral membrane proteins.

RESULTS

U21 exits from the Golgi in punctate vesicles distinct from MPR

In preparation for using the RUSH method to examine the progression of U21 through the secretory pathway, we fused U21 to SBP and either GFP or mCherry (Figure 1b). To ensure that fusion of the ~30-kDa RUSH tag to U21 did not alter the function of U21, we examined the U21-RUSH fusion protein's ability to reroute class I MHC molecules in HeLa cells. While properly folded class I MHC molecules reside on the cell surface of control HeLa cells (Figure 1c), in U21-expressing HeLa cells, U21 mediates characteristic relocalization of class I MHC molecules to perinuclear puncta, which were previously shown to colocalize with lamp1 and lamp2 in lysosomes (Figure 1e) (Hudson *et al.*, 2001; Glosson and Hudson, 2007). U21 colocalizes with the class I MHC molecules it reroutes (Figure 1f). In cells expressing the U21-RUSH (U21-SBP-mCherry) fusion protein in the presence of biotin, class I MHC molecules are relocalized to a punctate perinuclear location that is essentially indistinguishable from class I MHC molecules in nontagged U21-expressing cells, demonstrating that the RUSH-tagged U21 molecules retain their ability to reroute class I MHC molecules (Figure 1, e–h).

We next employed RUSH to examine transport of newly synthesized U21 and class I MHC molecules (HLA-A2) through the early secretory system. We also analyzed exit of various other reporter molecules from the Golgi region (Figure 1b, schematic). Before biotin addition, reporter proteins were retained in the ER; 3–4 min after addition of biotin to release of the reporter from the li hook, we observed the retained reporters localized in a reticular pattern characteristic of ER (Figure 2, a, e, l, and m; Supplemental Videos 1–4). Twenty to 35 min after biotin addition, we observed an accumulation of the reporter molecules in the Golgi region (Figure 2, b, f, j, and n).

To begin our examination of U21 exit from the Golgi, we first recapitulated RUSH using lamp1-SBP-GFP and SBP-GFP-CDMPR (Chen *et al.*, 2017). When we expressed lamp1-SBP-GFP in HeLa cells, the SBP-GFP-tagged lamp1 molecules exited the Golgi via tubular structures, and when we expressed SBP-GFP-CDMPR, the SBP-GFP-tagged CDMPR molecules exited in punctate vesicles (Figure 2, g and h, arrowheads, and Supplemental Video 2), just as described by Chen *et al.* (2017). When we expressed SBP-GFP-CDMPR, the SBP-GFP-tagged CDMPR molecules exited in punctate vesicles (Figure 2, g and h, arrowheads, and Supplemental Video 2) (Chen *et al.*, 2017). We next examined the trafficking of class I MHC molecules (HLA-A2-SBP-GFP). Because class I MHC molecules, like TfR, reside at the plasma membrane at the steady state, we expected that HLA-A2 reporter proteins would also exit the Golgi in tubules. As anticipated, RUSH-tagged HLA-A2-SBP-GFP molecules exited the Golgi in tubular carriers (Figure 2k, arrowheads, and Supplemental Video 3).

Lamp1, although destined for lysosomes, follows the indirect pathway to the plasma membrane and then travels through the endosomal system to lysosomes (for a review, see Obermüller *et al.*, 2002; Bralke and Bonifacino, 2009). Because we have seen that

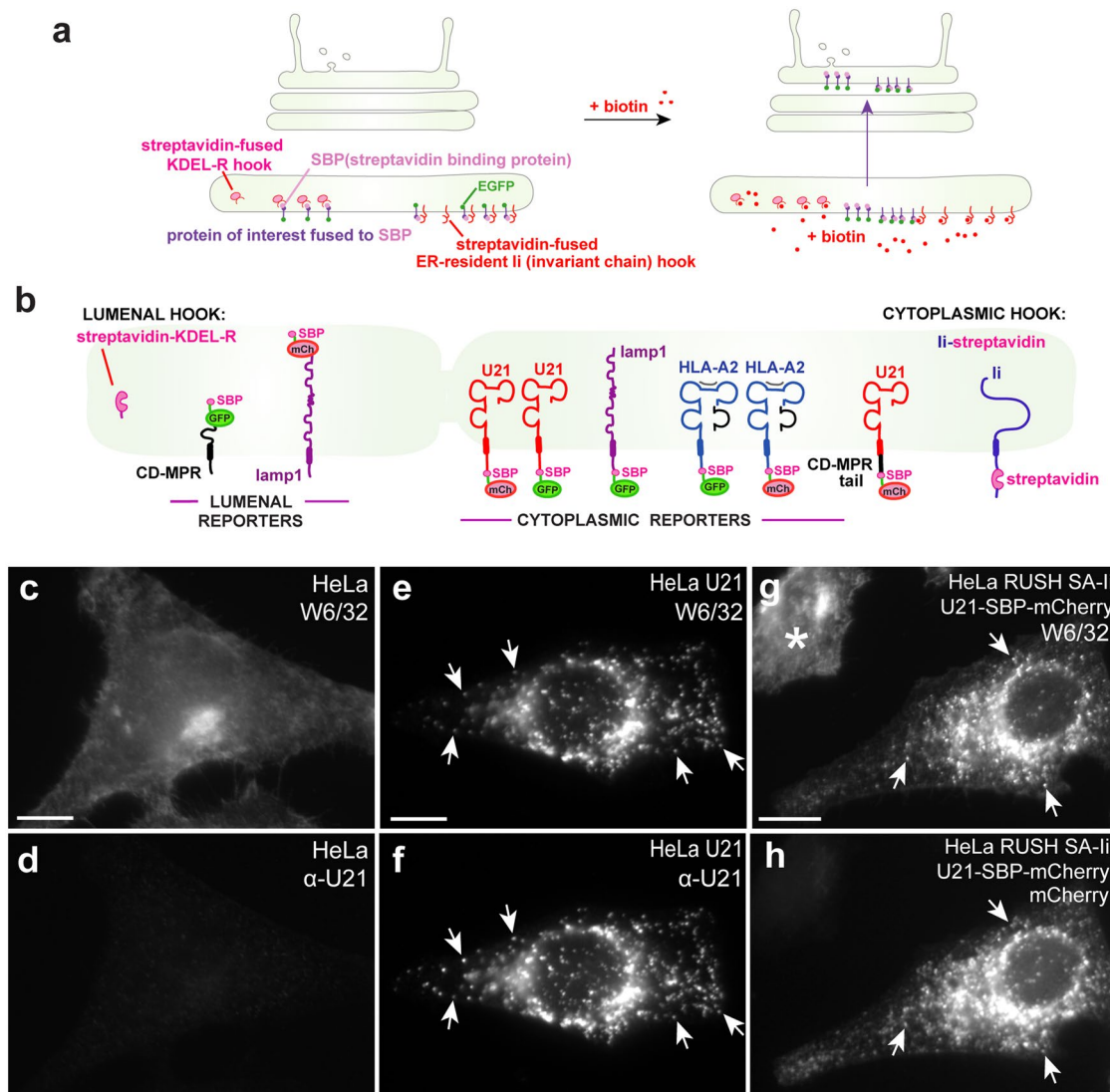


FIGURE 1: U21 RUSH. (a) RUSH: “hooks”—either the KDEL receptor or a mutant invariant chain fused to streptavidin—are expressed from a bicistronic plasmid also encoding a “reporter” protein of interest fused to SBP and either EGFP or mCherry. Biotin competitively releases the reporters from the hooks and monitoring of synchronous fluorescent reporter protein movement from the ER is performed. (b) Schematic of RUSH hooks and reporters used: the luminal KDEL-R hook was used for CDMPR and lamp1, as depicted. The cytoplasmic li hook was used for U21, lamp1, HLA-A2, and the U21-CDMPRTail chimera, as depicted. (c–h) Fusion of SBP and mCherry to U21 does not impair its ability to reroute class I MHC molecules in HeLa cells: epifluorescence microscopy of HeLa cells double labeled with an antibody directed against properly folded class I MHC (c, e, g) and U21-SBP-mCherry (d, f) in HeLa cells. Arrows denote coincident puncta. Asterisk denotes a cell that does not express U21-RUSH. Scale bars: 10 μm .

U21 also reaches the plasma membrane (Supplemental Figure S1), we hypothesized that U21 might travel with lamp1 from the Golgi in tubules. Surprisingly, U21-SBP-mCherry instead exited the Golgi in punctate vesicles (Figure 2o, arrows, and Supplemental Video 4). We therefore surmised that U21 must instead exit from the Golgi in the same vesicles as the CDMPR.

To examine the possibility that U21 exited from the Golgi in CDMPR-containing vesicular carriers, we coexpressed SBP-GFP-CDMPR and U21-SBP-mCherry. Each reporter protein was expressed using a bicistronic expression cassette to ensure proportional expression of their respective hooks (a KDEL hook for MPR and an li hook for U21). Approximately 90 min after biotin-induced release from their ER hooks, both SBP-GFP-CDMPR and U21-SBP-mCherry were seen to emerge from the Golgi in puncta. However,

the U21- and MPR-containing puncta did not colocalize, suggesting that U21 exits the Golgi in vesicles distinct from those of MPR and lamp1 (Figure 3 and Supplemental Video 5).

U21 segregates from CDMPR in the Golgi

To better visualize exit of U21 and CDMPR from the Golgi, we employed superresolution live imaging (3D-structured illumination microscopy [3D-SIM]) of the Golgi complex from cells coexpressing the SBP-GFP-CDMPR and U21-SBP-mCherry RUSH fusion proteins. We began imaging at ~20 min after biotin addition, allowing the RUSH-tagged proteins to arrive in the Golgi and become concentrated there. Approximately 26 min after biotin addition, U21-SBP-mCherry and SBP-GFP-CDMPR were largely colocalized in the Golgi stacks (Figure 4, a–c, and Supplemental Video 6). At 32 min, we

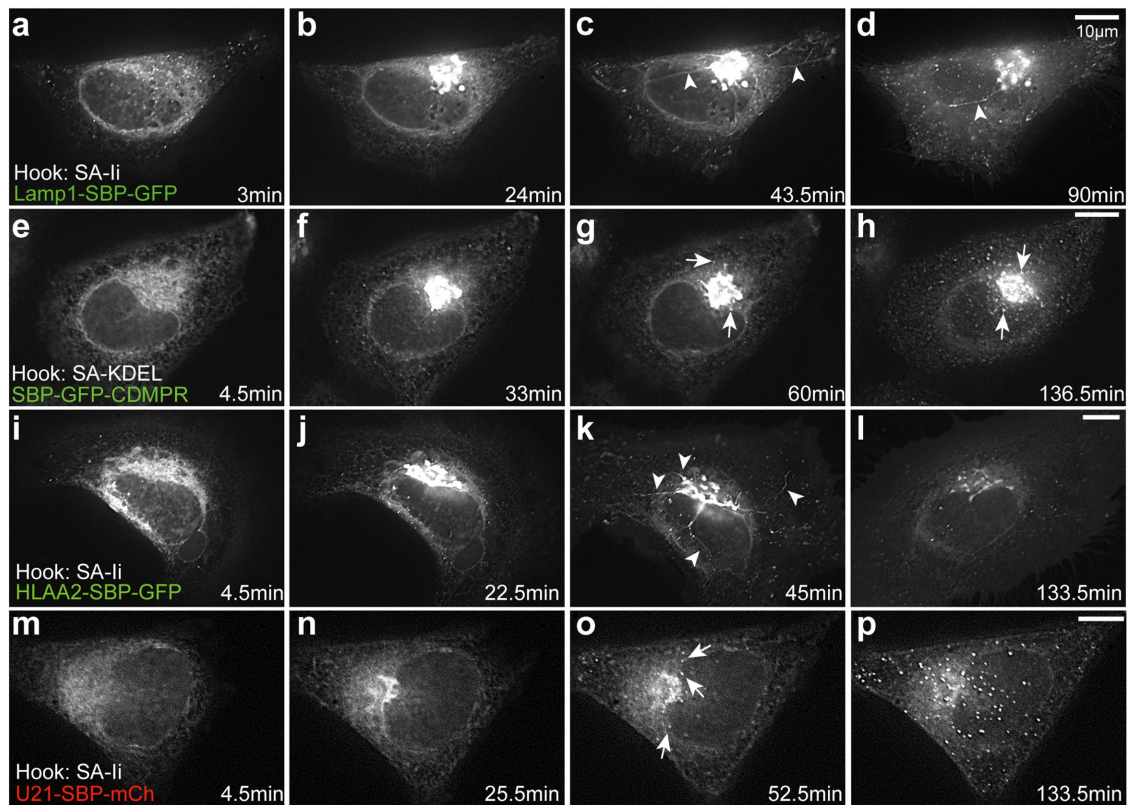


FIGURE 2: U21 exits from the Golgi in punctate vesicles. Live imaging of RUSH in HeLa cells transfected with plasmids encoding Lamp1-SBP-GFP (a–d), SBP-GFP-CDMPR (e–h), HLA-A2-SBP-GFP (i–l), and U21-SBP-mCherry (m–p), as noted. Still images were extracted from Supplemental Videos 1–4 at the indicated times after biotin addition. Reporter proteins were visualized exiting from the Golgi in tubules (arrowheads) or vesicles (arrows). Scale bars: 10 μ m.

observed segregation of U21-SBP-mCherry into regions of the Golgi distinct from that of SBP-GFP-CDMPR; where concentrated U21 existed, there was no CDMPR fluorescence (Figure 4, d–f, white arrowheads), as if U21 had segregated itself within the Golgi stack. Six minutes later, the concentrated U21-SBP-mCherry could be seen budding from the Golgi (Figure 4, j–l, yellow arrowheads).

U21-containing vesicles are larger than CDMPR-containing vesicles

We noted that the U21-SBP-mCherry-containing vesicles appeared larger than the SBP-GFP-CDMPR-containing vesicles. To examine whether a significant size difference exists between U21-SBP-mCherry- and SBP-GFP-CDMPR-containing vesicles, we measured the area and perimeter of U21-SBP-mCherry- and SBP-GFP-CDMPR-containing vesicles from three independent experiments. On average, U21-SBP-mCherry-containing vesicles were approximately 28% larger than SBP-GFP-CDMPR-containing vesicles, averaging 270 nm in diameter, compared with 210 nm for SBP-GFP-CDMPR-containing vesicles (Figure 5). These values are comparable in size to Golgi-derived CDMPR vesicles described by others (Polishchuk *et al.*, 2000; Hossain *et al.*, 2014). To ensure that the properties of the different fluorescent tags were not the cause of this apparent size difference, we exchanged the fluorescent proteins fused to U21 and CDMPR and confirmed that the fluor did not alter the measured area of the vesicles (Supplemental Figure S2).

U21-containing vesicles lack clathrin coats

The tubular plasma membrane–destined carriers that carry lamp1 lack clathrin coats, while vesicular CDMPR-containing carriers are

clathrin coated (Pols *et al.*, 2013; Chen *et al.*, 2017). U21-SBP-GFP-containing carriers are not tubular; thus, we hypothesized that, like the vesicular CDMPR carriers, the U21-SBP-GFP-containing carriers might possess clathrin coats. To test this hypothesis, we released the RUSH-tagged fusion proteins (U21-SBP-GFP or SBP-GFP-CDMPR) from the ER with biotin, and to maximize our chances of visualizing Golgi-derived carriers, we waited until just after the synchronized fusion proteins had begun to exit the Golgi (60 min after biotin addition) before fixing the cells and immunolabeling with an anti-clathrin antibody (Figure 6, a–f). SBP-GFP-CDMPR-containing vesicles near the Golgi appeared to colocalize in the center of clathrin-decorated puncta (Figure 6, a–c), while U21-SBP-GFP and clathrin did not appear at all colocalized (Figure 6, d–f), suggesting that Golgi-derived U21-containing vesicles are clathrin independent.

In addition to clathrin, cargo sorting of the dileucine motif-containing MPRs from the TGN involves recruitment of cargo adaptor proteins (GGAs) and AP-1 (Puertollano *et al.*, 2001; Doray *et al.*, 2002; Ghosh *et al.*, 2003; Mardones *et al.*, 2007). To further establish the distinction between CDMPR-containing carriers and U21-containing carriers, we released the RUSH-tagged fusion proteins (U21-SBP-GFP or SBP-GFP-CDMPR) from the ER with biotin as described earlier, and this time immunolabeled the cells with antibodies directed against GGA3 and AP-1 γ (Supplemental Figure S3, a–l). Because GGA1 and GGA3 colocalize with each other in the TGN (Ghosh *et al.*, 2003; Mardones *et al.*, 2007) and depletion of GGA3 has been shown to alter CI-MPR localization (Ghosh *et al.*, 2003; Puertollano and Bonifacino, 2004), we examined GGA3. As expected, RUSH-tagged SBP-GFP-CDMPR-containing vesicles near the Golgi appeared to colocalize with GGA3, while RUSH-tagged

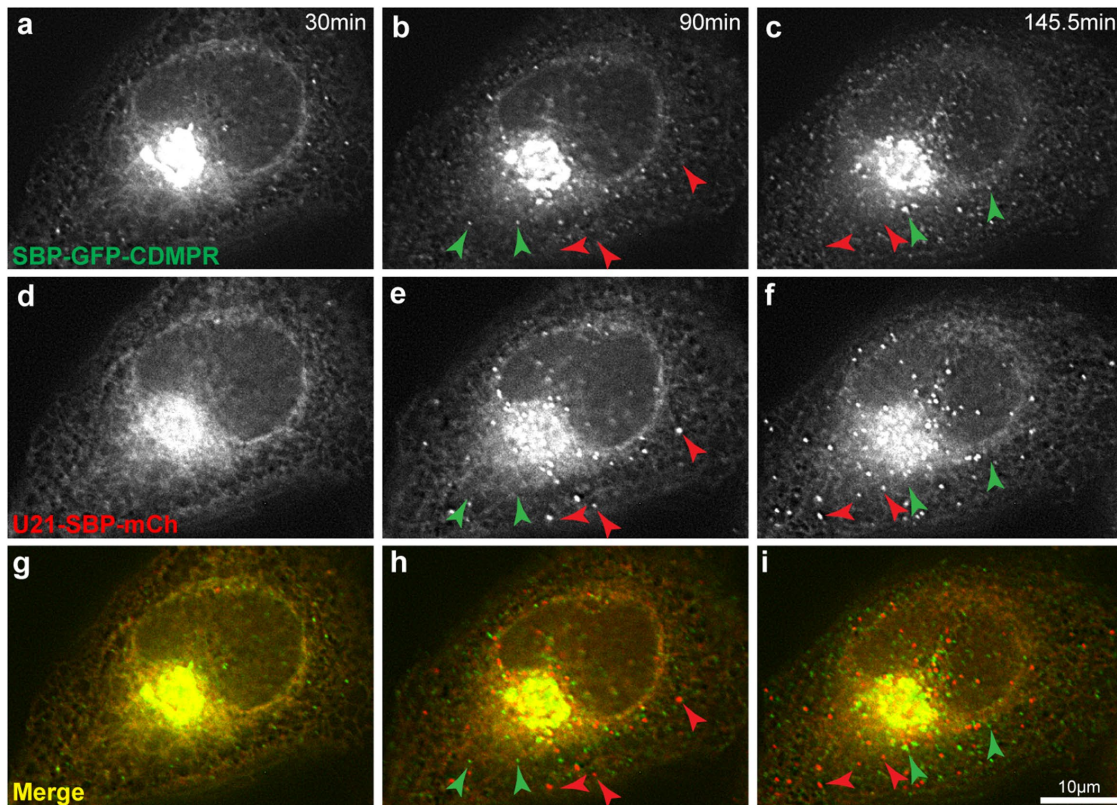


FIGURE 3: U21 and CDMPR leave the Golgi in distinct punctate carriers. Live imaging of RUSH in HeLa cells cotransfected with plasmids encoding SBP-GFP-CDMPR (a–c) and U21-SBP-mCherry (d–f). Still images were extracted from movies at the indicated times after biotin addition. (g–i) Merged images. Green arrowheads indicate the position of CDMPR-containing vesicles. Red arrowheads indicate the position of U21-containing vesicles. Scale bar: 10 μm .

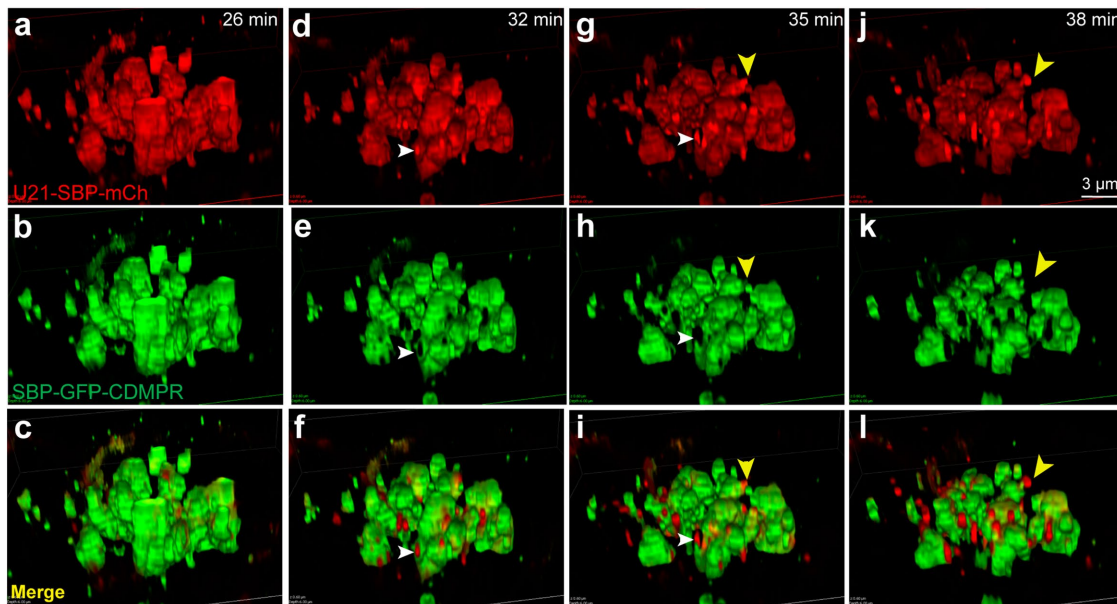


FIGURE 4: U21 segregates from CDMPR in the Golgi. Live imaging of RUSH in HeLa cells expressing RUSH U21 (U21-SBP-mCh) and RUSH CDMPR (SBP-GFP-CDMPR). Reporter molecules were released from their hooks with biotin and superresolution imaging was performed at 3-min intervals after both proteins had reached the Golgi. Still images were extracted from the movie at the indicated times after biotin addition. (c, f, i, l) Merged images. White arrowheads in d–i show U21-SBP-mCherry segregating from SBP-GFP-CDMPR in the Golgi (d, g) and absence of SBP-GFP-CDMPR from sites of U21-SBP-mCherry concentration (e, h). (f, i) Merged images. Yellow arrowhead (g–l) shows a budding U21-containing carrier devoid of SBP-GFP-CDMPR. Scale bar: 3 μm .

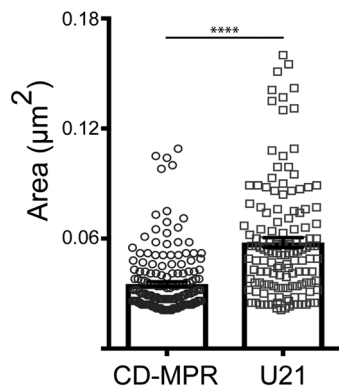


FIGURE 5: U21-containing vesicles are larger than CDMPR-containing vesicles. HeLa cells expressing U21-SBP-mCherry (circles) and SBP-GFP-CDMPR (squares) reporter proteins were incubated with biotin for 45–60 min. Cells were fixed, and images were acquired on a structured illumination microscope. U21- ($n = 137$) and CDMPR-positive ($n = 175$) vesicles were measured from three or four independent experiments. **** = significant to $p < 0.0001$. Bars show mean \pm SEM. U21: 0.058 mm^2 vs. CDMPR: 0.035 mm^2 . $\sim 271 \text{ nm}$ vs. $\sim 212 \text{ nm}$ in diameter.

U21-SBP-GFP did not (Supplemental Figure S3, a–f). Likewise, RUSH-tagged SBP-GFP-CDMPR-containing vesicles colocalized with AP-1 γ , while RUSH-tagged U21-SBP-GFP did not (Supplemental Figure S3, g–i). These results, which are quantitated in Supplemental Figure S3m, further substantiate our conclusion that Golgi-derived U21-containing vesicles are clathrin-, AP-1-, and GGA3-independent and distinct from MPR-containing carriers.

The cytoplasmic tail of CDMPR is not enough to influence segregation of U21 from CDMPR

The cytoplasmic tail of CDMPR contains a DXXLL motif that recruits the GGA clathrin adaptor proteins. These adaptor proteins help to recruit clathrin and mediate sorting of CDMPR from the Golgi to an endosomal compartment (for review, see Brulke and Bonifacio, 2009). The cytoplasmic tail of U21 lacks a canonical DXXLL motif. Moreover, the cytoplasmic tail of U21 is not necessary for its trafficking to the lysosomal compartment (Hudson *et al.*, 2003). To assess whether the well-characterized sorting signals contained within the CDMPR tail could exert influence over the segregation of U21 into the larger, distinct, U21-containing Golgi exit carriers, we constructed RUSH chimeras between U21 and CDMPR, replacing the cytoplasmic tail of U21 with that of CDMPR, hypothesizing that the cytoplasmic tail of CDMPR would suffice to direct the U21-CDMPRTail chimera to clathrin-coated CDMPR-containing vesicles (see Figure 1b, schematic). To visualize U21-CDMPRTail-SBP-GFP molecules after exit from the Golgi, we released the U21-CDMPRTail-SBP-GFP chimeric molecules from the ER with biotin and again waited until just after the synchronized fusion proteins had begun to exit the Golgi (60 min after biotin addition) before fixing the cells and immunolabeling them with anti-clathrin antibody. Surprisingly, the U21-CDMPRTail-SBP-GFP fusion did not appear to colocalize with clathrin (Figure 6, g–j). We also measured the size of the U21-CDMPRTail-SBP-GFP-containing puncta and found them to be similar in size to U21-SBP-GFP-containing puncta, significantly larger than SBP-GFP-CDMPR-containing puncta (Figure 6k). These results suggest that recruitment of GGA and clathrin to the U21-CDMPRTail chimera was not sufficient to influence the segregation of U21-CDMPRTail into distinct U21-containing carriers.

U21 and class I MHC molecules traffic together from the Golgi in vesicles

U21 binds to class I MHC molecules within minutes after synthesis in the ER and reroutes them to the lysosomal compartment (Hudson *et al.*, 2001). We would therefore expect that U21-RUSH (U21-SBP-GFP) should bind to and reroute RUSH-tagged HLA-A2 (HLA-A2-SBP-mCherry) molecules when both reporter proteins are expressed in the same cell. As we demonstrated, HLA-A2-SBP-GFP exits the Golgi in tubules and traffics to the plasma membrane when U21 is not also present (Figure 2k and Supplemental Video 3). When we coexpress both HLA-A2-SBP-mCherry and U21-SBP-GFP and monitor their traffic through the secretory pathway, HLA-A2-containing tubules are absent, and all vesicles that contain U21 also contain HLA-A2 (Figure 7 and Supplemental Video 7). This important result demonstrates that the RUSH-fused U21-SBP-GFP molecules are functional and that RUSH-tagged HLA-A2-SBP-mCherry molecules bind to U21 and are efficiently segregated into U21-containing Golgi carriers by U21.

TGN46 segregates from U21

Wakana *et al.* (2012) have described another type of Golgi transport carrier, called CARTS (carriers of the TGN to the cell surface). These plasma membrane–destined Golgi-derived carriers were isolated from a membrane fraction enriched in TGN46, an integral membrane protein that traffics from the TGN to the plasma membrane (Rajasekaran *et al.*, 1994; Ponnambalam *et al.*, 1996; Banting and Ponnambalam, 1997). Like U21-containing carriers, CARTS also exclude VSV-G, which travels to the plasma membrane in tubular carriers (Chen *et al.*, 2017). We therefore hypothesized that U21 could be transported in CARTS. To assess this possibility, we expressed RUSH-tagged U21 (U21-SBP-GFP) in HeLa cells, released the U21-SBP-GFP with biotin, and allowed the synchronized proteins to begin to exit from the Golgi before fixing the cells and immunolabeling them with an anti-TGN46 antibody. TGN46, which is predominantly localized to the TGN, could also be seen in small puncta throughout the cell (Figure 8b). U21-SBP-GFP-containing carriers, however, were significantly larger and distinct from these TGN46-positive puncta, suggesting that U21-containing carriers are not CARTS (Figure 8, a–d).

U21 exits the Golgi with small molecule–controlled oligomers

Induced oligomerization of Golgi-resident integral membrane proteins has been shown to trigger exit of these oligomers from the Golgi in punctate carriers that then traffic to lysosomes for degradation (Tewari *et al.*, 2015). To induce oligomerization of integral membrane proteins, Tewari and colleagues fused three tandem FKBP12 (FM) domains to the cytoplasmic tails of the Golgi-resident integral membrane proteins galactosyl transferase (GalT) and mannosidase I (ManI) (Rizzo *et al.*, 2013; Tewari *et al.*, 2015). FM domains self-associate, and these GalT-FM and ManI-FM molecules were shown to oligomerize in the Golgi. Once oligomerized, the oligomers exited the Golgi in vesicular carriers and were degraded in a lysosomal compartment (Rizzo *et al.*, 2013; Tewari *et al.*, 2015). In the presence of a cell-permeable small molecule that disrupts FM-FM interactions, the FM-fused oligomers become monomeric. Monomeric GalT-FM behaves like endogenous GalT and resides in the *trans*-Golgi (Rizzo *et al.*, 2013; Tewari *et al.*, 2015).

We have previously shown that U21 binds to class I MHC molecules in a 4:2 ratio and forms heterohexameric or dodecameric oligomers *in vitro*, thus the possibility that U21 might exit from the Golgi in carriers that also include oligomerized proteins was enticing

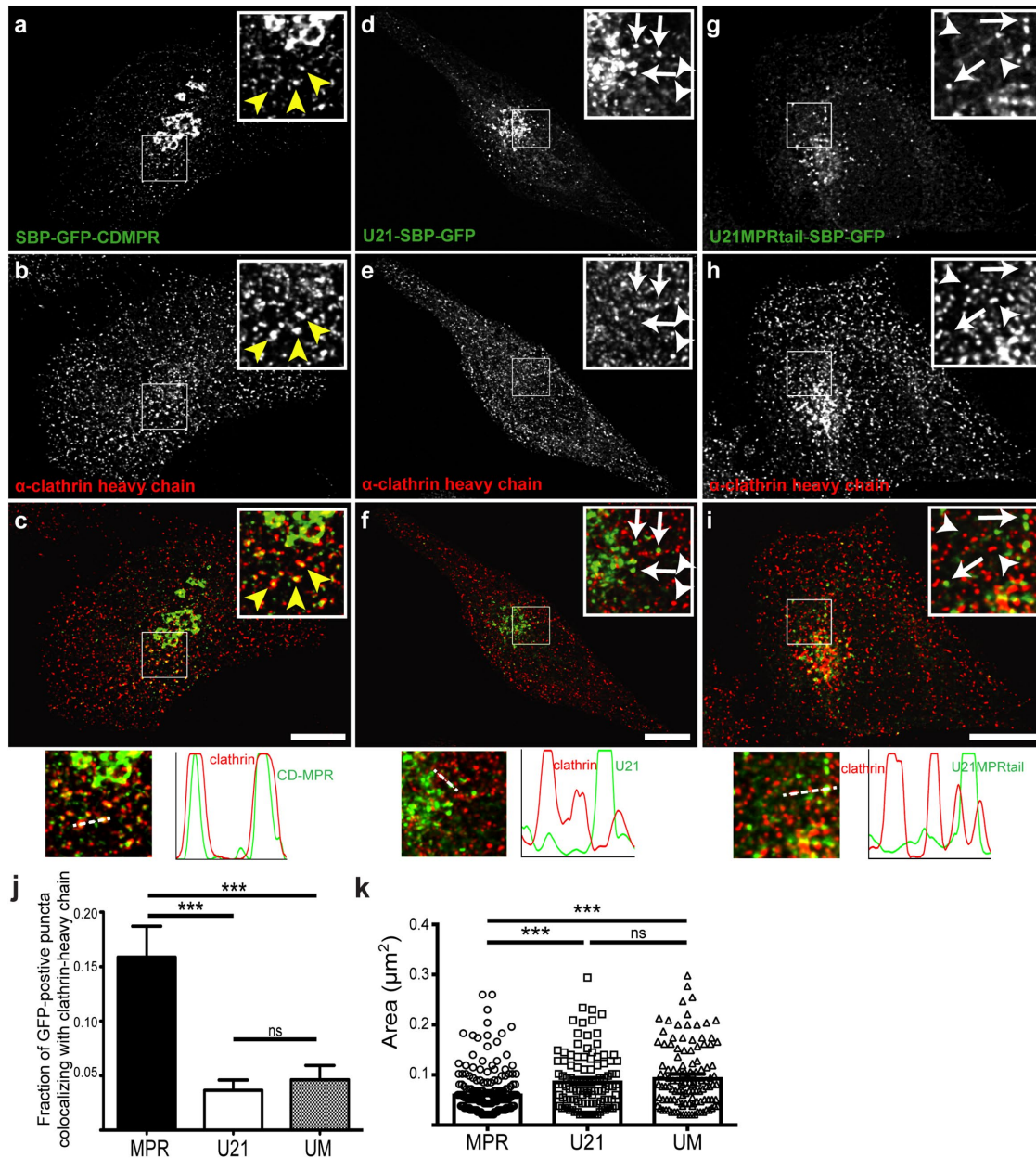


FIGURE 6: U21-containing carriers do not colocalize with clathrin. Confocal colocalization of CDMPR or U21 with clathrin heavy-chain molecules in HeLa cells expressing either SBP-GFP-CDMPR (a–c), U21-SBP-GFP (d–f), or U21-MPRtail-SBP-GFP (g–i). Cells were incubated with biotin for 60 min and then fixed and labeled with antibody directed against clathrin heavy chain. Enlarged views are depicted in boxed regions. (a–c) Yellow arrowheads indicate points of colocalization between SBP-GFP-CDMPR (green) and clathrin (red). (d–f) Arrows indicate U21-SBP-GFP–positive puncta. Arrowheads indicate clathrin heavy-chain–positive puncta. (g–i) A chimeric U21-MPRtail-SBP-GFP fusion protein was expressed in HeLa cells and incubated with biotin as in a–f. Arrows indicate U21-MPRtail-SBP-GFP–containing puncta and arrowheads point out clathrin heavy-chain–positive puncta. Merged images and plots of fluorescence intensity through the white dashed lines are shown at the bottom. (j, k) Colocalization with α -clathrin heavy-chain (j) and quantification of vesicle size (k). Circles and white bar, SBP-GFP-CDMPR; squares and black bar, U21-SBP-GFP; triangles and gray bar, U21-MPRtail-SBP-GFP. Scale bar in a–i: 10 μm . ns = not significant, *** = significant to $p < 0.001$.

(May *et al.*, 2014). To examine the possibility that U21 exits the Golgi in carriers that also include inducibly oligomerized proteins, we performed an experiment in cells coexpressing RUSH-tagged U21-SBP-mCherry and GalT-FM fused to GFP (GalT-FM-GFP) (Tewari *et al.*, 2015). GalT-FM-GFP, when monomerized using the small molecule “D/D solubilizer,” behaves like endogenous GalT and resides in the *trans*-Golgi (Rizzo *et al.*, 2013; Tewari *et al.*, 2015). Within

60 min of D/D solubilizer washout, the GalT-FM-GFP molecules form homo-oligomers that exit the Golgi in punctate carriers (Tewari *et al.*, 2015).

To synchronize release of GalT-FM-GFP and U21-SBP-mCherry, we transfected HeLa cells with the two constructs in the presence of D/D solubilizer and then washed out D/D solubilizer in medium containing biotin. The biotin released U21-SBP-mCherry from its ER

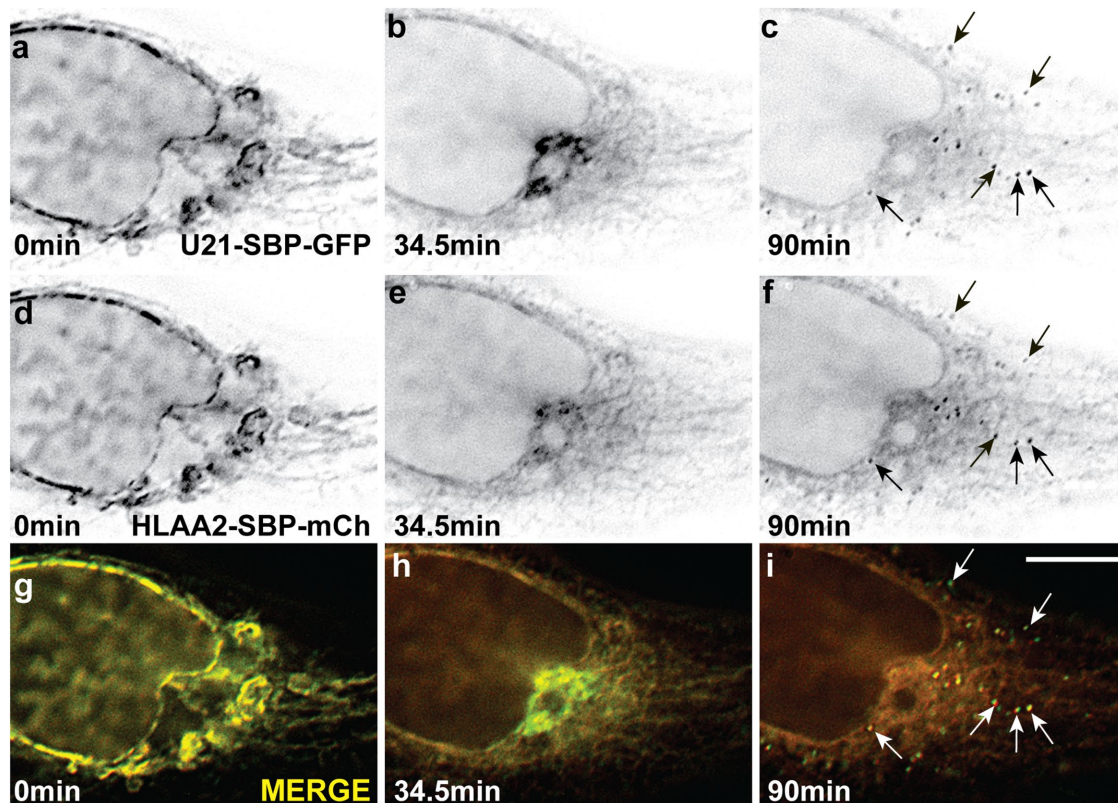


FIGURE 7: U21 and class I MHC molecules colocalize in vesicular carriers. Live imaging of RUSH in HeLa cells expressing U21-SBP-GFP (a–c) and HLA-A2-SBP-mCherry (d–f). Still images were extracted from movies at the indicated times after biotin addition. (g–i) Merged images. Arrows indicate coincident vesicular carriers in U21 and HLA-A2 images. Scale bar: 10 μ m.

tether, while the washout of D/D solubilizer induced oligomerization of GalT-FM-GFP molecules in the *trans*-Golgi, resulting in segregation of GalT-FM-GFP into lysosome-destined carriers. Although these molecules are synchronously released from different points in the secretory pathway, and the release of each protein requires different molecular events to induce their exit, the exit of each molecule from the Golgi continues over a period of at least 2 h; thus, if the two fluorescent fusion proteins segregated into the same Golgi exit carriers, we hypothesized that we might observe overlap and colocalization of a portion of GalT-FM-GFP and U21-SBP-mCherry during the 2-h period after release.

Thirty minutes after washout and biotin addition, we observed colocalization of U21-SBP-mCherry with GalT-FM-GFP. Colocalization continued for the duration of the imaging experiment (Figure 9 and Supplemental Video 8). GalT-FM-GFP is highly concentrated in the Golgi, and while not every GalT-FM-GFP-positive carrier contained U21-SBP-mCherry, most U21-SBP-mCherry-positive carriers were GalT-FM-GFP-positive (Figure 9, arrows). We note that, in this experiment, the relatively long exposure times of \sim 400 ms, coupled with the time it took to move the filter cube turret was long enough to prevent appearance of complete colocalization of these dynamic carriers. Video images, however, show that each punctate carrier moves in the same direction at the same speed, reducing concern about whether the two fluoros are coincident. This coincidence is even more striking when considering the complete absence of CDMPR, lamp1, clathrin, or TGN46 in U21-containing exit carriers (Figures 3, 4, 6, and 8; for lamp1, unpublished data). We therefore hypothesize that U21 exit carriers are the same as carriers used by aggregated GalT-FM-GFP, a hypothesis that is strengthened by our

observation that, unlike CDMPR carriers, GalT-FM-GFP-containing carriers were not significantly different in size from U21-SBP-GFP carriers (Supplemental Figure S4).

DISCUSSION

Chen *et al.* (2017) demonstrated that that RUSH-fused transmembrane proteins destined for the endolysosomal compartment are segregated into distinct Golgi domains before export into two distinct transport carriers—either tubules (for lamp1 and plasma membrane-destined cargo) or vesicles (for direct sorting of MPR to the endolysosomal pathway). Our results build on their data to demonstrate that the lysosome-destined U21 immunoevasin from HHV-7 segregates from both CDMPR and lamp1 in the Golgi to be exported in a third type of Golgi carrier—a larger, clathrin-independent vesicular carrier distinct from that used by CDMPR (see model, Figure 9f).

At the outset of these experiments, we hypothesized that U21 would exit the Golgi with lamp1, in tubules, given that its steady-state localization so closely mirrors that of lamp1, and because we were able to detect the presence of U21 on the cell surface and subsequent internalization in clathrin-coated vesicles. We note, however, that while depletion of the clathrin adaptor protein complex AP-2 resulted in accumulation of lamp1 on the cell surface (Janvier and Bonifacino, 2005), depletion of AP-2 from U21-expressing cells had little effect upon class I MHC or U21 localization, suggesting that U21 may not use the indirect pathway to lysosomes to the same extent as lamp1 (Kimpler *et al.*, 2014). Our results here clearly demonstrate that U21 and lamp1 do not share the same mode of exit from the Golgi.

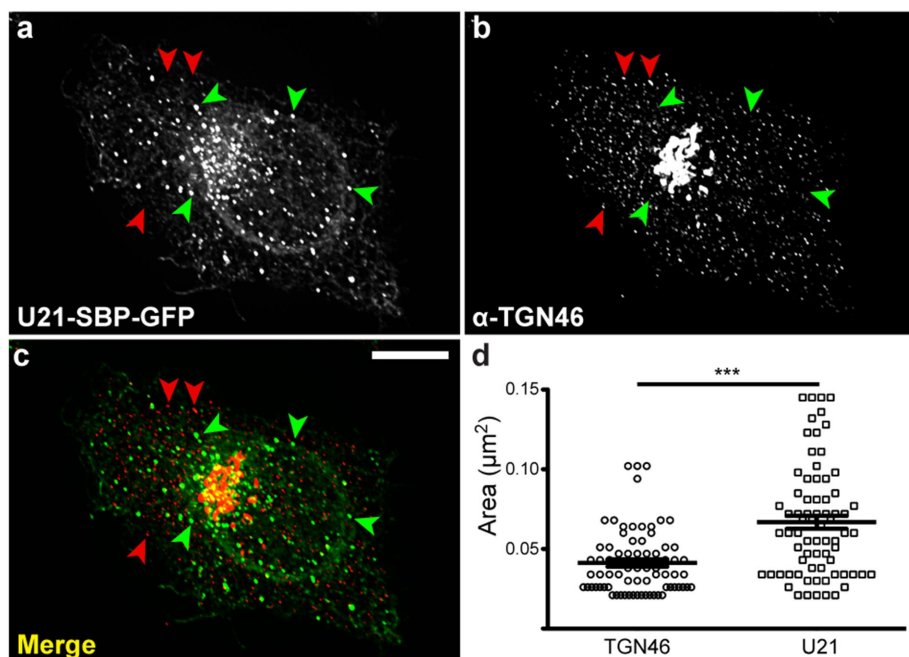


FIGURE 8: U21 does not colocalize with TGN46. (a) HeLa cells expressing U21-SBP-GFP reporter molecules were incubated with biotin for 55 min and then fixed and labeled with antibody directed against TGN-46 (b). (c) Merged image: green arrowheads indicate U21-containing puncta; red arrowheads indicate TGN-46-containing puncta. Scale bar: 10 μm . (d) The areas of U21-SBP-GFP-containing puncta ($n = 74$) and TGN46-positive puncta ($n = 73$) were measured from six different cells and two independent experiments. U21-SBP-GFP: 0.067 mm^2 vs. CARTS: 0.041 mm^2 . Vesicle sizes were compared by one-way analysis of variance with a Newman-Keuls multiple-comparison test applied to show significance. Lines represent the means. Error bars reflect SEM; *** = significant to $p < 0.001$.

To exit the Golgi en route to an endosomal compartment, CDMPR and sortilin each contain a DXXLL sequence in their cytoplasmic tails that recruits GGAs (Puertollano *et al.*, 2001). CDMPR also binds to the clathrin adaptor AP-1 at the TGN for entry into clathrin-coated endosome-destined carrier vesicles (for review, see Braulke and Bonifacino, 2009). The cytoplasmic tail of U21 lacks a canonical DXXLL motif. Moreover, we have previously shown that the cytoplasmic tail of U21 is not necessary for its trafficking to the lysosomal compartment (Hudson *et al.*, 2003). To assess the relative influence of the cytoplasmic tail of CDMPR in governing segregation into CDMPR-containing carriers, we hypothesized that, if we substituted the cytoplasmic tail of CDMPR for U21's cytoplasmic tail, the U21-CDMPR tail fusion protein would be recruited into sortilin- and CDMPR-containing Golgi exit carriers. Surprisingly, U21 trafficking was unaffected by the well-characterized sorting signals in the CDMPR tail, suggesting either that the luminal domain of U21 exerts a dominant influence on its sorting into its novel Golgi exit carriers or that U21 associates with a cellular protein that exerts a dominant influence on its sorting. Interestingly, we have previously shown that depletion of AP-1 and AP-3 adaptor molecules alter U21's ability to reroute class I MHC molecules to the lysosomal compartment (Kimpler *et al.*, 2014). Here, however, we demonstrate that AP-1 is not present on U21-containing carriers as they exit from the Golgi. We speculate that U21's dependence on AP-1 to reroute class I MHC molecules to lysosomes may be the result either of other cellular proteins critical for U21 function that depend on AP-1, or of a dependence on AP-1 that occurs after exit from the Golgi.

Is the U21-containing carrier a novel Golgi exit carrier, or is this carrier established solely for the trafficking of U21? While it is

possible that expression of U21, a class I MHC-like viral transmembrane protein, can by itself induce the formation of a novel vesicle carrier destined for lysosomes, we think it more likely that the virus has evolved to appropriate a preexisting cellular Golgi carrier vesicle for its own use. If so, what might be the normal cellular cargo carried in this distinct U21-containing vesicular Golgi carrier?

Wakana *et al.* (2012) have described another type of Golgi-derived transport carrier, called CARTS. Like U21-containing carriers, CARTS exclude VSV-G (Wakana *et al.*, 2012), which has long been observed to exit the Golgi in tubules (Hirschberg *et al.*, 1998; Toomre *et al.*, 1999; Polishchuk *et al.*, 2003). We therefore hypothesized that CARTS may be the U21-containing carrier. However, we demonstrate here that TGN46, the flagship member of CARTS, does not colocalize with U21, suggesting that U21-containing carriers are distinct from CARTS.

How could the luminal domain of U21 provide the information required to segregate it away from tubular or clathrin-dependent CDMPR-containing carriers? One attractive hypothesis to explain U21's ability to segregate into lysosome-destined carriers in the Golgi is that the U21-containing carriers are the result of the formation of an oligomeric complex of U21 and class I molecules that is too large or too ordered to

be segregated into Golgi-derived tubular carriers: we have previously demonstrated that U21 binds to class I MHC molecules as a tetramer, forming 4:2 heterohexamers and dodecamers with purified class I MHC molecules (May *et al.*, 2014). U21/class I MHC oligomers might be segregated into cellular carriers containing oligomeric or aggregated proteins destined for lysosomes. Precedent exists for this idea: Weflen *et al.* (2013) have suggested that the neonatal Fc receptor, which, like U21, is also a class I-fold-containing MHC-like molecule, travels to lysosomes when it is cross-linked at the plasma membrane, possibly because it cannot enter endocytic tubules. Indeed, receptor cross-linking at the cell surface might be a general method to trigger internalization and lysosomal targeting of class I MHC molecules (Moody *et al.*, 2015).

While our data suggest that U21's clustering effect upon class I molecules occurs in the Golgi and not at the plasma membrane, we propose the idea that oligomerization of class I and U21 promotes segregation and exclusion of these oligomers from plasma membrane-destined tubular carriers in the Golgi. This segregation event must take precedence over GGA- and clathrin-mediated formation of CDMPR-containing carriers, because replacing U21's cytoplasmic tail with the cytoplasmic tail of CDMPR did not alter U21's segregation into U21-containing carriers. Wolins *et al.* (1997) proposed a similar model for the sorting of furin, demonstrating that the luminal domain of furin forms aggregates in the TGN that traffic to lysosomes. In addition, Tewari and colleagues have more recently described manganese-dependent clustering and rerouting of the Golgi-resident integral membrane protein GPP130 to lysosomes. Sorting of GPP130 clusters to lysosomes is dependent on sortilin and GGA, however, and we have shown that U21-containing carriers

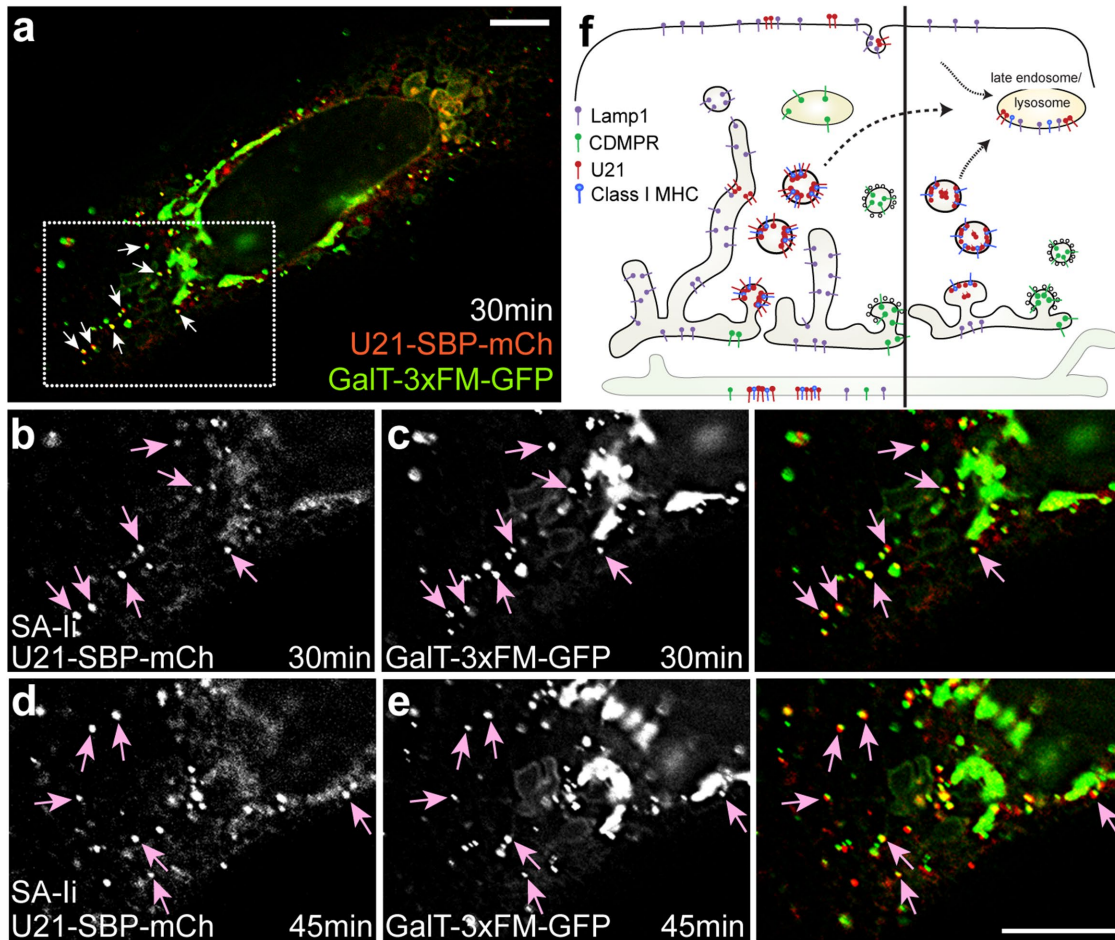


FIGURE 9: U21 exits from the Golgi with inducibly oligomerized GalT-FM. Live imaging of HeLa cells transfected with plasmids encoding U21-SBP-mCherry and GalT-3xFM-GFP. Still-image enlargements of the box in a were extracted from movies at the indicated times after simultaneous biotin addition and D/D solubilizer washout. Points of colocalization between U21 (b, d) and GalTFM (c, e) are illustrated (arrows). Merged images are shown on the right. (f) Model: U21 (red) exits from the Golgi in vesicular carriers distinct from the clathrin-coated vesicles containing sortilin and CDMPR (green) or the tubules that carry lamp1 (purple) (modified from Chen *et al.*, 2017). Left, U21 tetramers associate with class I MHC molecules (blue) in a 4:2 ratio soon after synthesis and are segregated into QC carriers in the late Golgi. Some U21 escapes QC carriers and is seen at the plasma membrane. Right, Soluble U21 also associates with class I MHC molecules and reroutes them to lysosomes. Illustration depicts fewer cytoplasmic tails accessible to act as signal marking oligomeric integral membrane proteins. Scale bars: 10 μ m.

are distinct from the clathrin-coated CDMPR/sortilin/GGA-containing carriers (Puertollano *et al.*, 2001; Tewari *et al.*, 2014, 2015).

The solution to the mystery of how U21 so effectively reroutes class I MHC molecules to lysosomes finally becomes apparent when viewed in the context of recent data by Venkat and Linstedt (2017), which demonstrated that, while oligomers of GPP130 exited the Golgi with GGA and sortilin, FM-fused GalT oligomers exited the Golgi in a sortilin-independent carrier. Interestingly, Hellerschmied *et al.* (2019) have recently demonstrated that inducibly-oligomerized FM-GalT cargo exits from the Golgi in carriers that also transport inducibly unfolded proteins. They term these carriers "quality control (QC) carriers" (Hellerschmied *et al.*, 2019). Here, our use of RUSH to monitor U21 as it progresses through the secretory pathway has led to the discovery of a clathrin-independent Golgi carrier, devoid of TGN-46, CDMPR, and lamp1, but containing FM-GalT. We therefore propose that the mechanism by which the HHV-7 U21 protein so effectively reroutes class I MHC molecules to lysosomes is through formation of U21/class I MHC oligomers that exit the

Golgi en route to lysosomes using cellular QC carriers. This novel viral mechanism for eliminating class I MHC molecules provides new biological context for the function of QC carriers, which have been shown to carry proteins engineered to aggregate via oligomerization domains and proteins engineered to unfold in the presence of chemical inducers (Rizzo *et al.*, 2013; Venkat and Linstedt, 2017; Hellerschmied *et al.*, 2019).

How might oligomeric proteins be segregated away from lamp1 and CDMPR/sortilin-containing carriers? One possibility is that the arrangement of oligomeric/aggregated proteins within the plane of the Golgi membrane may create an ordered or planar region of membrane that segregates itself from nonoligomeric integral membrane proteins. Membrane curvature indicative of aggregated integral membrane proteins might then be detected by either cytosolic or luminal proteins (McMahon and Boucrot, 2015; Hellerschmied *et al.*, 2019). Interestingly, U21 reroutes class I MHC molecules to lysosomes even when it is expressed as a soluble secreted protein lacking its transmembrane domain and cytoplasmic tail, suggesting that

recognition of clustered integral membrane proteins occurs from the luminal side of the Golgi membrane or that oligomers containing only the cytoplasmic tails of class I MHC molecules are sufficient for segregation (Hudson *et al.*, 2003; May *et al.*, 2014) (Figure 9f).

Is the segregation of U21 oligomers and unfolded proteins into distinct exit carriers the “default” pathway? Our experiment replacing the cytoplasmic tail of U21 with that of CDMPR demonstrated that the U21-CDMPRTail fusion protein did not enter clathrin-coated CDMPR carriers, suggesting both that segregation of U21 is dependent on the luminal domain of U21 and that segregation of U21 occurs earlier than or is dominant over the sorting of CDMPR into GGA/clathrin-coated carriers. The formation of QC carriers may therefore be the result of an active sorting event. Alternatively, the arrangement of oligomeric or aggregated integral membrane proteins may preclude their entrance into any other pathway, despite even the presence of canonical sorting signals contained within their cytoplasmic tails.

In summary, we propose that HHV-7 U21 has evolved a novel mechanism to divert class I MHC molecules to lysosomes, forming U21-class I MHC oligomers that result in their segregation into distinct Golgi-derived clathrin-independent QC carriers destined for lysosomes. We are now poised to pursue identification of distinguishing elements of these carriers that are required for their formation and for their trafficking to lysosomes.

MATERIALS AND METHODS

Cell lines, antibodies and reagents

HeLa cells (generously provided by Peter Howley, Harvard Medical School, Boston, MA), were cultured in DMEM (Invitrogen, Carlsbad, CA) supplemented with 5% fetal bovine serum (FBS) and 5% newborn calf serum. The cells were tested for mycoplasma using 4',6-diamidino-2-phenylindole and PCR, as previously described (Uphoff and Drexler, 2002, 2011; Young *et al.*, 2010). Stable expression of U21 was carried out using lentivirus-mediated gene transfer, using the vector pHAGE-Puro-MCS, which carries a selectable marker for puromycin resistance (Mostoslavsky *et al.*, 2006; May *et al.*, 2010). The monoclonal antibody W6/32 recognizes assembled, β 2m-associated class I MHC molecules (Barnstable *et al.*, 1978). The polyclonal antibody MCW62 (U21-N) was raised against the N-terminus of HHV-7 U21 (May *et al.*, 2014). The monoclonal antibody H3B4, directed against lamp1, was generously provided by T. August (Johns Hopkins, Baltimore, MD) (Mane *et al.*, 1989). The monoclonal anti-clathrin heavy-chain antibody X22 was purchased from Thermo Scientific (cat. no. MA1-065). The monoclonal antibody directed against AP1- γ (100/3) was generously provided by T. Kirchhausen, Harvard Medical School (Ahle *et al.*, 1988). The monoclonal antibody directed against GGA3 (clone 8) was obtained from BD Biosciences (cat. no. 612310). Alexa Fluor 488-, Alexa Fluor 594-, and Alexa Fluor 647-conjugated goat-anti-mouse and rabbit secondary antibodies were used at dilutions recommended by the manufacturer (Thermo Scientific, Waltham, MA). Chemicals were purchased from Sigma Millipore (St. Louis, MO) unless otherwise noted.

Recombinant DNA

Bicistronic RUSH plasmids encoding the mutant invariant chain hook and lamp1 reporter protein fused to SBP and EGFP were generously provided by F. Perez and G. Boncompain (Curie Institute, Paris, France) (Boncompain and Perez, 2012). Plasmid constructs to synchronize the traffic of the U21 (UniProt accession no. P60505) and HLA-A2 (GenBank accession no. U18930.1) were generated by replacing sequences encoding the reporter proteins in the original bicistronic RUSH cassette constructs, in which a mutant streptavidin-

fused invariant chain (CD74) was used as the hook (Boncompain and Perez, 2012). GFP or mCherry and SBP were fused to the cytoplasmic tails of U21, HLA-A2, and CDMPR using the restriction enzyme sites included within the modular RUSH cassette (Boncompain and Perez, 2012). Bicistronic RUSH plasmids using the KDEL hook with CDMPR and LAMP1 were generously provided by J. Bonifacio (National Institute of Child Health and Human Development, National Institutes of Health, Bethesda, MD). The pEGFP-N3-based GalT-FM construct, described in Tewari *et al.* (2015), was generously provided by Adam Linstedt (Carnegie Mellon University, Pittsburgh, PA).

Transient transfection of RUSH constructs

For live-cell imaging experiments, 1.3×10^5 HeLa cells were plated onto glass-bottom dishes (MatTek, Ashland, MA; cat. no. P35G-1.5-20-C) coated with 5 μ g/ml fibronectin (MilliporeSigma Burlington, MA; cat. no. fc010) 1 d before transfection. Cells were transfected using FuGENE6 (Promega, Madison, WI; cat. no. E2691). RUSH-tagged constructs were released with D-biotin (Amresco, Solon, OH; cat. no. 3040) at a final concentration of 40 μ M. For the GalT-FM release experiment, HeLa cells were transfected with both RUSH U21-SBP-mCherry and GalT-3xFM-GFP and incubated in the presence of D/D solubilizer (1 μ M) (Takara, Mountain View, CA; cat. no. 635054) (Tewari *et al.*, 2015), which prevents aggregation of FM-domain-containing proteins. For visualizing synchronous release of GalT-FM and RUSH U21-SBP-mCherry, D/D solubilizer-containing medium was removed from the plate and replaced with complete medium (10% FBS) containing 40 μ M biotin and lacking phenol red.

Immunofluorescence

For capturing release of the RUSH reporters from the Golgi, HeLa cells on coverslips were transfected with U21-SBP-GFP or SBP-GFP-CDMPR (FuGENE6 or Transporter5, Polysciences, Warrington, PA; cat. no. 26008). RUSH reporters U21-SBP-GFP or SBP-GFP-CDMPR were released from the ER with biotin (40 μ M) for 20 min at 37°C and then fixed in 4% paraformaldehyde. Cells were then washed with phosphate-buffered saline (PBS) and permeabilized with 0.5% saponin + 3% bovine serum albumin (BSA; Gemini BioProducts, West Sacramento, CA; cat. no. 700-100P) before being labeled with primary and then Alexa Fluor-conjugated secondary antibodies. All steps were performed in 0.5% saponin + 3% BSA, with the exception of three final PBS washes. For colocalization of GGA3 with U21-SBP-GFP or SBP-GFP-CDMPR, cells were instead fixed in methanol for 15 min at -20°C. For colocalization of clathrin with internalized α -U21 and α -class I MHC, Zenon-647 IgG1 (Invitrogen Z25008) was used to label α -clathrin heavy chain (X22).

Fluorescence microscopy

Images of GalT were captured using a Nikon Eclipse Ti Microscope System equipped with NIS-Elements AR imaging software (v. 4.60). Images were taken using a Nikon 60 \times oil-immersion lens (Plan Apo VC, 1.4 NA) and a Photometrics CoolSnap EZ CCD camera and deconvolved using Nikon deconvolution software (v. 4.40). Superresolution microscopy was performed on a Nikon Structured-Illumination Microscope (N-SIM; Nikon) using NIS-Elements AR imaging and 3D reconstruction software (v. 5.11). SIM images were taken using a heated Nikon 100 \times oil-immersion lens (CFI Apo SR TIRF, 1.49 NA) and an Andor iXon+897 EMCCD camera. Live-cell images on the SIM were captured every 3 min, beginning 20 min after biotin addition. Confocal microscopy was performed on a Nikon Eclipse Ti2 microscope equipped with a W1 Spinning Disc, Orca Flash CMOS camera, and 60 \times oil-immersion objective

(CFI Plan Apo λ , 1.4 NA), and NIS-Elements AR imaging and 3D reconstruction software (v. 6.0). All microscopes were equipped with motorized stages, Tokei Hit environmental chambers (temperature-controlled at 37°C and 5% CO₂), and Nikon Perfect Focus motors. Live-cell images were captured every 90 s, beginning just after biotin addition. Video and still images were deconvoluted using Nikon Elements deconvolution software (v. 4.51, 5.11, or 6), exported as TIF files, and cropped using Adobe Photoshop CS5 (Adobe, San Jose, CA).

Quantification and data analysis

Line analysis of deconvolved images was performed using the public domain Fiji image-processing package (Schindelin *et al.*, 2012; Schneider *et al.*, 2012; Rueden *et al.*, 2017). U21- and CDMPR-containing vesicles were quantitated from HeLa cells expressing the RUSH reporters as described in Figure 3. RUSH reporters (U21 and CDMPR) were released from their ER hooks with biotin and fixed for 45–60 min after biotin addition. To increase the likelihood of quantifying Golgi-derived vesicles, a 10 × 10 μm^2 region of interest was drawn to include a small region of the Golgi. Images were cropped using Nikon Elements software (v. 5.11). The cropped images were then imported into FIJI using the Bio-Formats importer (Linkert *et al.*, 2010). A polygonal selection was used to exclude the Golgi from further analysis. Gaussian blur (5.00 Sigma) was used to remove background from the image, and a threshold was set to include the top 1% of pixels. Object size was measured, constrained with an area restriction between 0.02 and 0.30 μm^2 and a circularity between 0.5 and 1.0. Measurements for area, perimeter, and Feret's diameter were determined using FIJI. In each experiment, vesicles were measured in two to six cells. An unpaired two-tailed Student's *t* test was performed using GraphPad Prism5. Data are shown as mean \pm SEM. For all experiments, at least three independent experiments were performed.

For quantification of colocalization of GFP-tagged RUSH constructs with clathrin heavy chain, AP1, and GGA3, vesicles were counted and analyzed for colocalization as described by Omari *et al.* (2018). Three 10 × 10 μm^2 boxes were randomly placed around the Golgi, and a threshold was placed on the top 3% of pixels for each protein signal. AP-1 or GGA3 vesicles were first counted using the FIJI Analyze Particles function with a 0.02–0.30 size restriction and a 0.5–1.0 circularity threshold. The resulting AP-1 or GGA3 mask was then applied to the threshold image of RUSH-U21 or RUSH-MPR images using the “AND” command to show only overlapping fluorescence. The resulting image was counted using the Analyze Particles function with the restrictions described earlier. The number of vesicles counted from the “AND” image were divided by the number of total vesicles counted from the AP1 or GGA3 threshold image, yielding the percent of GFP-positive vesicles.

ACKNOWLEDGMENTS

This work was supported by National Institutes of Health grant RO1-GM120735 and Supplemental Award to A.W.H. We thank Gaelle Boncompain and Franck Perez (Curie Institute, Paris, France) for kind provision of the original RUSH constructs and advice; Juan Bonifacino and David Gershlick (National Institute of Child Health and Human Development, National Institutes of Health, Bethesda, MD) for generous provision of their modified RUSH constructs; Adam Linstedt (Carnegie Mellon University, Pittsburgh, PA) for helpful discussion and generous provision of GalT-3XFM construct; Adriano Marchese and Tom Kirchhausen for generous provision of antibodies; and Paula Traktman, Nancy Dahms, Mark McNally, and members of the Hudson lab for helpful discussion and critical review of the article.

REFERENCES

- Ahle S, Mann A, Eichelsbacher U, Ungewickell E (1988). Structural relationships between clathrin assembly proteins from the Golgi and the plasma membrane. *EMBO J* 7, 919–929.
- Alcami A, Koszinowski UH (2000). Viral mechanisms of immune evasion. *Trends Microbiol* 8, 410–418.
- Banting G, Ponnambalam S (1997). TGN38 and its orthologues: roles in post-TGN vesicle formation and maintenance of TGN morphology. *Biochim Biophys Acta* 1355, 209–217.
- Bard F, Malhotra V (2006). The formation of TGN-to-plasma-membrane transport carriers. *Annu Rev Cell Dev Biol* 22, 439–455.
- Barnstable CJ, Bodmer WF, Brown G, Galfre G, Milstein C, Williams AF, Ziegler A (1978). Production of monoclonal antibodies to group A erythrocytes, HLA and other human cell surface antigens—new tools for genetic analysis. *Cell* 14, 9–20.
- Boncompain G, Divoux S, Gareil N, de Forges H, Lescure A, Latreche L, Mercanti V, Jollivet F, Raposo G, Perez F (2012). Synchronization of secretory protein traffic in populations of cells. *Nat Methods* 9, 493–498.
- Boncompain G, Perez F (2012). Synchronizing protein transport in the secretory pathway. *Curr Protoc Cell Biol Chapter 15:Unit 15.19*.
- Braulke T, Bonifacino JS (2009). Sorting of lysosomal proteins. *Biochim Biophys Acta* 1793, 605–614.
- Chen Y, Gershlick DC, Park SY, Bonifacino JS (2017). Segregation in the Golgi complex precedes export of endolysosomal proteins in distinct transport carriers. *J Cell Biol* 8, jcb.201707172.
- Doray B, Ghosh P, Griffith J, Geuze HJ, Kornfeld S (2002). Cooperation of GGAs and AP-1 in packaging MPRs at the trans-Golgi network. *Science* 297, 1700–1703.
- Douglas JL, Gustin JK, Viswanathan K, Mansouri M, Moses AV, Früh K (2010). The great escape: viral strategies to counter BST-2/tetherin. *PLoS Pathog* 6, e1000913.
- Ghosh P, Griffith J, Geuze HJ, Kornfeld S (2003). Mammalian GGAs act together to sort mannose 6-phosphate receptors. *J Cell Biol* 163, 755–766.
- Glosson NL, Gonyo P, May NA, Schneider CL, Ristow LC, Wang Q, Hudson A (2010). Insight into the mechanism of human herpesvirus 7 U21-mediated diversion of class I MHC molecules to lysosomes. *J Biol Chem* 285, 37016–37029.
- Glosson NL, Hudson A (2007). Human herpesvirus-6A and -6B encode viral immunoevasins that downregulate class I MHC molecules. *Virology* 365, 125–135.
- Hellerschmied D, Serebrenik YV, Shao L, Burslem GM, Crews CM (2019). Protein folding state-dependent sorting at the Golgi apparatus. *Mol Biol Cell* 30, 2296–2308.
- Hirschberg K, Miller CM, Ellenberg J, Presley JF, Siggia ED, Phair RD, Lippincott-Schwartz J (1998). Kinetic analysis of secretory protein traffic and characterization of Golgi to plasma membrane transport intermediates in living cells. *J Cell Biol* 143, 1485–1503.
- Hossain T, Riad A, Siddiqi S, Parthasarathy S, Siddiqi SA (2014). Mature VLDL triggers the biogenesis of a distinct vesicle from the trans-Golgi network for its export to the plasma membrane. *Biochem J* 459, 47–58.
- Hudson A, Blom D, Howley PM, Ploegh HL (2003). The ER-luminal domain of the HHV-7 immunoevasin U21 directs class I MHC molecules to lysosomes. *Traffic* 4, 824–837.
- Hudson A, Howley PM, Ploegh HL (2001). A human herpesvirus 7 glycoprotein, U21, diverts major histocompatibility complex class I molecules to lysosomes. *J Virol* 75, 12347–12358.
- Hunziker W, Geuze HJ (1996). Intracellular trafficking of lysosomal membrane proteins. *Bioessays* 18, 379–389.
- Janvier K, Bonifacino JS (2005). Role of the endocytic machinery in the sorting of lysosome-associated membrane proteins. *Mol Biol Cell* 16, 4231–4242.
- Kimpler LA, Glosson NL, Downs D, Gonyo P, May NA, Hudson A (2014). Adaptor protein complexes AP-1 and AP-3 are required by the HHV-7 immunoevasin U21 for rerouting of class I MHC molecules to the lysosomal compartment. *PLoS One* 9, e99139.
- Kornfeld S, Mellman I (1989). The biogenesis of lysosomes. *Annu Rev Cell Biol* 5, 483–525.
- Linkert M, Rueden CT, Allan C, Burel J-M, Moore W, Patterson A, Loranger B, Moore J, Neves C, MacDonald D, *et al.* (2010). Metadata matters: access to image data in the real world. *J Cell Biol* 189, 777–782.
- Mane SM, Marzella L, Bainton DF, Holt VK, Cha Y, Hildreth JE, August JT (1989). Purification and characterization of human lysosomal membrane glycoproteins. *Arch Biochem Biophys* 268, 360–378.

- Mardones GA, Burgos PV, Brooks DA, Parkinson-Lawrence E, Mattera R, Bonifacino JS (2007). The *trans*-Golgi network accessory protein p56 promotes long-range movement of GGA/clathrin-containing transport carriers and lysosomal enzyme sorting. *Mol Biol Cell* 18, 3486–3501.
- May NA, Glosson NL, Hudson A (2010). HHV-7 U21 downregulates classical and nonclassical class I major histocompatibility complex molecules from the cell surface. *J Virol* 84, 3738–3751.
- May NA, Wang Q, Balbo A, Konrad SL, Buchli R, Hildebrand WH, Schuck P, Hudson A (2014). Human herpesvirus-7 U21 tetramerizes to associate with class I major histocompatibility complex molecules. *J Virol* 88, 3298–3308.
- McMahon HT, Boucrot E (2015). Membrane curvature at a glance. *J Cell Sci* 128, 1065–1070.
- Moody PR, Sayers EJ, Magnusson JP, Alexander C, Borri P, Watson P, Jones AT (2015). Receptor crosslinking: a general method to trigger internalization and lysosomal targeting of therapeutic receptor:ligand complexes. *Mol Ther* 23, 1888–1898.
- Mostoslavsky G, Fabian AJ, Rooney S, Alt FW, Mulligan RC (2006). Complete correction of murine Artemis immunodeficiency by lentiviral vector-mediated gene transfer. *Proc Natl Acad Sci USA* 103, 16406–16411.
- Obermüller S, Kiecke C, von Figura K, Höning S (2002). The tyrosine motifs of Lamp 1 and LAP determine their direct and indirect targeting to lysosomes. *J Cell Sci* 115, 185–194.
- Omari S, Makareeva E, Roberts-Pilgrim A, Mirigian L, Jarnik M, Ott C, Lippincott-Schwartz J, Leikin S (2018). Noncanonical autophagy at ER exit sites regulates procollagen turnover. *Proc Natl Acad Sci USA* 115, E10099–E10108.
- Polishchuk EV, Di Pentima A, Luini A, Polishchuk RS (2003). Mechanism of constitutive export from the Golgi: bulk flow via the formation, protrusion, and en bloc cleavage of large *trans*-Golgi network tubular domains. *Mol Biol Cell* 14, 4470–4485.
- Polishchuk RS, Polishchuk EV, Marra P, Alberti S, Buccione R, Luini A, Mironov AA (2000). Correlative light-electron microscopy reveals the tubular-saccular ultrastructure of carriers operating between Golgi apparatus and plasma membrane. *J Cell Biol* 148, 45–58.
- Pols MS, van Meel E, Oorschot V, ten Brink C, Fukuda M, Swetha MG, Mayor S, Klumperman J (2013). hVps41 and VAMP7 function in direct TGN to late endosome transport of lysosomal membrane proteins. *Nat Commun* 4, 1361.
- Ponnambalam S, Girotti M, Yaspo ML, Owen CE, Perry AC, Suganuma T, Nilsson T, Fried M, Banting G, Warren G (1996). Primate homologues of rat TGN38: primary structure, expression and functional implications. *J Cell Sci* 109, 675–685.
- Puertollano R, Aguilar RC, Gorshkova I, Crouch RJ, Bonifacino JS (2001). Sorting of mannose 6-phosphate receptors mediated by the GGAs. *Science* 292, 1712–1716.
- Puertollano R, Bonifacino JS (2004). Interactions of GGA3 with the ubiquitin sorting machinery. *Nat Cell Biol* 6, 244–251.
- Rajasekaran AK, Humphrey JS, Wagner M, Miesenböck G, Le Bivic A, Bonifacino JS, Rodriguez-Boulant E (1994). TGN38 recycles basolaterally in polarized Madin-Darby canine kidney cells. *Mol Biol Cell* 5, 1093–1103.
- Rizzo R, Parashuraman S, Mirabelli P, Puri C, Lucocq J, Luini A (2013). The dynamics of engineered resident proteins in the mammalian Golgi complex relies on cisternal maturation. *J Cell Biol* 201, 1027–1036.
- Rueden CT, Schindelin J, Hiner MC, DeZonia BE, Walter AE, Arena ET, Eliceiri KW (2017). ImageJ2: ImageJ for the next generation of scientific image data. *BMC Bioinformatics* 18, 529.
- Schindelin J, Arganda-Carreras I, Frise E, Kaynig V, Longair M, Pietzsch T, Preibisch S, Rueden C, Saalfeld S, Schmid B, et al. (2012). Fiji: an open-source platform for biological-image analysis. *Nat Methods* 9, 676–682.
- Schneider CA, Rasband WS, Eliceiri KW (2012). NIH Image to ImageJ: 25 years of image analysis. *Nat Methods* 9, 671–675.
- Tewari R, Bachert C, Linstedt AD (2015). Induced-oligomerization targets Golgi proteins for degradation in lysosomes. *Mol Biol Cell* 26, 4427–4437.
- Tewari R, Jarvela T, Linstedt AD (2014). Manganese induces oligomerization to promote down-regulation of the intracellular trafficking receptor used by Shiga toxin. *Mol Biol Cell* 25, 3049–3058.
- Toomre D, Keller P, White J, Olivo JC, Simons K (1999). Dual-color visualization of *trans*-Golgi network to plasma membrane traffic along microtubules in living cells. *J Cell Sci* 112, 21–33.
- Tortorella D, Gewurz BE, Furman MH, Schust DJ, Ploegh HL (2000). Viral subversion of the immune system. *Annu Rev Immunol* 18, 861–926.
- Uphoff CC, Drexler HG (2002). Comparative PCR analysis for detection of mycoplasma infections in continuous cell lines. *In Vitro Cell Dev Biol Anim* 38, 79–85.
- Uphoff CC, Drexler HG (2011). Detecting mycoplasma contamination in cell cultures by polymerase chain reaction. *Methods Mol Biol* 731, 93–103.
- Venkat S, Linstedt AD (2017). Manganese-induced trafficking and turnover of GPP130 is mediated by sortilin. *Mol Biol Cell* 28, 2569–2578.
- Wakana Y, van Galen J, Meissner F, Scarpa M, Polishchuk RS, Mann M, Malhotra V (2012). A new class of carriers that transport selective cargo from the *trans* Golgi network to the cell surface. *EMBO J* 31, 3976–3990.
- Weflen AW, Baier N, Tang Q-J, Van den Hof M, Blumberg RS, Lencer WI, Massol RH (2013). Multivalent immune complexes divert FcRn to lysosomes by exclusion from recycling sorting tubules. *Mol Biol Cell* 24, 2398–2405.
- Wolins N, Bosshart H, Küster H, Bonifacino JS (1997). Aggregation as a determinant of protein fate in post-Golgi compartments: role of the luminal domain of furin in lysosomal targeting. *J Cell Biol* 139, 1735–1745.
- Young L, Sung J, Stacey G, Masters JR (2010). Detection of *Mycoplasma* in cell cultures. *Nat Protoc* 5, 929–934.
- Zhu Y, Doray B, Poussa A, Lehto VP, Kornfeld S (2001). Binding of GGA2 to the lysosomal enzyme sorting motif of the mannose 6-phosphate receptor. *Science* 292, 1716–1718.